

Probing new physics with high-multiplicity events: Ultrahigh-energy cosmic rays at air-shower detector arrays

Yongsoo Jho^{*} and Seong Chan Park[†]

Department of Physics and IPAP, Yonsei University, Seoul 03722, Republic of Korea

(Dated: May 27, 2022)

Semi-classical processes such as production and decay of electroweak sphaleron in the Standard Model and also microscopic black hole in low scale gravity scenario typically involve large number of particles in final states. These large multiplicities can be distinctively seen in collisions of Ultrahigh-energy cosmic rays (UHECRs) with $E_{CR} \gtrsim 10^9$ GeV and nucleons in the atmosphere of the Earth. Focusing on air-shower detector array experiments including Telescope Array Experiment (TA) and Pierre-Auger Observatory (Auger), we propose strategic ways to discover and analyze such events.

I. INTRODUCTION

Recent observation of Ultra-High-Energy cosmic rays (UHECRs) extended the domain of the high-energy frontier covering beyond the reach of collider experiments. Many $\mathcal{O}(10)$ EeV cosmic ray events and a few $\mathcal{O}(1)$ PeV neutrino events have been already observed by ground air-shower detector arrays [1, 2] and other large detectors [3]. There are widely accepted and also more speculative potential origins of such UHECRs: young magnetized neutron star [4], active galactic nuclei (AGN) [5], gamma-ray burst (GRB) [6, 7], BL Lac type objects [8], dark matter and topological defects [9] but none of them has been confirmed yet. Furthermore, the fluxes, composition and the production mechanisms of UHECRs sensitively depend on the origin. Thus they still need to be clarified [10–15].

Even though uncertainties are still persist, our attention focuses on scattering process of UHECR with *known* targets such as the nucleons in the atmosphere. We anticipate that such ‘fixed-target’ experiment can provides a testing ground for particle physics beyond TeV scale [16]. Indeed the collision energy can be as high as $\sqrt{m_N E_{CR}} = \mathcal{O}(1 - 100)$ TeV given that the energy of the colliding cosmic ray particle is around $\mathcal{O}(1)$ PeV– $\mathcal{O}(10)$ EeV with the nucleon mass $m_N \simeq 1$ GeV.

As a concrete example of relevant physics showing only above 1 TeV, we focus on the electroweak sphaleron process in this paper. The sphaleron is predicted to take place at around 10 TeV in the standard model [17–22] but never has been experimentally tested and confirmed yet [23, 24]. We also study the microscopic blackholes predicted in low scale gravity scenarios for the hierarchy problem [25, 26].¹ The process of sphaleron and that of microscopic black hole share common properties such as large multiplicities and grown interaction cross sections at higher energies. We show that these common properties lead to observational consequences at the

air-shower detector array experiments such as Telescope Array Experiment (TA) and Pierre-Auger Observatory (Auger) [31–36].

The paper is organized as follows: in Sec. II, we discuss the cross sections of electroweak sphaleron and microscopic black hole events. In Sec. III, we discuss the event rates of new physics processes taking the GZK neutrino flux. In Sec. IV, we show noticeable phenomenological features for each case and discuss potential detection of new physics effects. The recently reported ‘muon deficits’ in hadronic interaction models [37–39] are also discussed. Finally, we conclude in Sec. V. The appendix includes all details of the calculations used in the paper.

II. PRODUCTION CROSS SECTIONS FOR SPHALERON AND BLACK HOLE

In this section, we discuss phenomenological details of the air-showers induced by electroweak sphaleron and microscopic black hole. The air-showers typically accompany with large multiplicity in signals. The showers are boosted so that the final-state particles are highly collinear and confined within a small separation angle $\delta\theta \sim \mathcal{O}(1/\gamma_{\text{boost}})$, where $\gamma_{\text{boost}} = 1/\sqrt{1-v^2}$ is the relativistic gamma factor of the produced particles with velocity v .

A. Parton level cross sections

The electroweak sphaleron is predicted within the standard model as a saddle point solution to the classical field equation of the electroweak gauge theory [17, 18]. It is a highly unstable configuration thus is not directly observable. However its decay products, the Standard Model gauge bosons [40] and fermions, leave observable effects [41] and reveal their presence in processes in the early universe. It also induces directly measurable signals in high energy collisions of UHE cosmic ray as we will closely study in this paper.

Sphaleron is involved in baryon number generation by inducing Chern-Simon (CS) number changing ($\Delta n_{\text{CS}} =$

^{*} jys34@yonsei.ac.kr

[†] sc.park@yonsei.ac.kr

¹ See [27] for a recent review on microscopic blackhole and [28–30] for quantum blackholes.

$\pm n$) and baryon number (B) and lepton number (L) violating ($\Delta(B+L) \neq 0$, $\Delta(B-L) = 0$) processes. The generated baryon and lepton numbers are quantized as $\Delta B = \Delta L = \pm 3n$, where $n \in \mathbb{Z}$ is an integer number. As the sphaleron process is effective in unbroken phase of electroweak symmetry, the baryon number, if generated before electroweak symmetry breaking, will be ‘wiped out’ by sphaleron processes [19, 20]. On the other hand, the generated lepton number is ‘converted’ into baryon numbers via sphaleron. Therefore, it is important in baryogenesis from the lepton number generation [20, 22].

Beside the role in baryogenesis, even though the sphaleron is robustly predicted *within* the Standard Model, it has never been experimentally tested due to the high sphaleron threshold at $E_{\text{sph}} \approx 10$ TeV. The UHE cosmic rays are particularly interesting since they reach this high threshold. According to recent works by Ellis and his collaborator [42, 43], the production cross section of Sphaleron in scattering of i and j initial partons can be relatively large²:

$$\hat{\sigma}_{ij \rightarrow \text{EWSph}}(E_{\text{CM}}) \simeq \frac{p}{m_W^2} \theta(E_{\text{CM}}/E_{\text{sph}}), \quad (1)$$

where $m_W = 80.38$ GeV, $\theta(x)$ is the Heaviside step function and an unknown parameter $p \lesssim 1$ encapsulates the unknown theoretical details. The cross section is not suppressed beyond the threshold because the sphaleron process is a collection of all possible processes over periodic vacua and the multiple contributions from all vacua overcome the exponential suppression factor [45, 46]. We take this cross section as a benchmark expression for the new physics ‘sphaleron’.

A microscopic black hole forms through collision of particles with a relatively low energy, $\sqrt{s} \gtrsim 1$ TeV, in low-energy gravity scenarios [25, 26]. Once produced, a microscopic black hole may explosively decay into multiple number of photons and also other Standard Model particles through Hawking radiation with high Hawking temperature, $T_{\text{Hawking}} > m_t$ [47, 48]. Thus the collision of UHE cosmic ray with a nucleon in the atmosphere is a potential source of a high-multiplicity event.

The parton level production cross section of ($i + j \rightarrow$ black hole + X) is approximately given as

$$\hat{\sigma}_{ij \rightarrow \text{BH}}(E_{\text{CM}}) \approx \pi (G_D E_{\text{CM}})^{\frac{2}{D-3}}, \quad (2)$$

where $G_D = 1/M_D^{D-2}$ is the gravitational constant in $D (= 4 + n)$ -dimensions with n -extra compact dimensions [25, 26, 49, 50]. The Schwarzschild radius is rapidly growing as $r_{\text{Sch}} \approx (G_D E)^{1/D-3}$ so that the resultant cross section grows too. Assuming $M_D \sim \text{TeV}$ in low energy gravity scenarios, the cross section can be sizable as $\hat{\sigma} \gtrsim 1/\text{TeV}^2$ when $E \gtrsim \text{TeV}$.

² See however, [44, 45]. Conventionally it has been believed that the production cross section of a sphaleron in particle collision is exponentially suppressed even when the collision energy is beyond the threshold [22], $\hat{\sigma}_{ij \rightarrow \text{Sphaleron}} \propto e^{-E/E_{\text{sph}}}$.

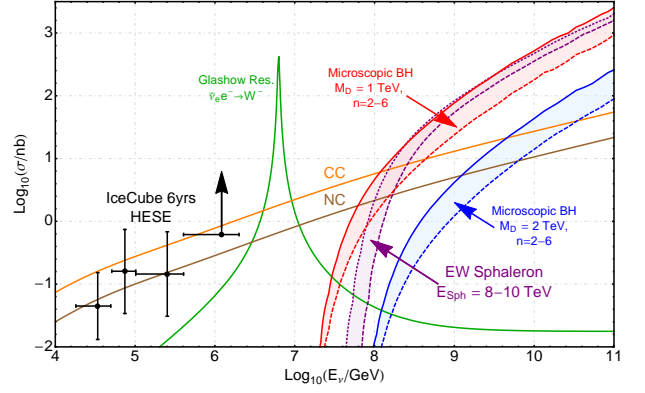


FIG. 1: **[Neutrino-induced cross sections with nucleon or electron.]** The CC/NC neutrino-nucleon deep-inelastic scattering (DIS) (orange and brown), Glashow resonance (green), electroweak sphaleron with $E_{\text{Sph}} = 8 - 10$ TeV (purple band), microscopic blackholes with $M_D = 1$ TeV (red band) and $M_D = 2$ TeV (blue band) for the number of compact dimensions, from $n = 2$ (bottom) to $n = 6$ (top). We fixed the ratio between the minimum energy for black hole production and the gravity scale as $x_{\text{min}} \equiv M_{\text{min}}/M_D = 5$ for all cases. The black dots with error bars are $\nu - N$ cross section obtained from the 6-years IceCube high-energy starting events (HESE) shower data set.

B. $\nu - N$ cross section

The $\nu - N$ cross section can be obtained by taking the parton distribution functions (PDF), $f_q(x, \hat{Q}^2)$, for a quark, q , in nucleon, N . The total cross sections for electroweak sphaleron and microscopic black hole are respectively given after the PDF convolution for nucleon:

$$\begin{aligned} \sigma_{\text{EWSph, BH}}^{\nu N}(E_{\text{lab}}) \\ = \int_{x_{\text{min}}}^1 dx f_q(x, 2xm_N E_{\text{lab}}) \hat{\sigma}_{\text{EWSph, BH}}^{\nu q}(\hat{s}), \end{aligned} \quad (3)$$

where $\hat{s} = 2xm_N E_{\text{lab}}$. The parton level cross sections are given in Eq. 1 and Eq. 2, respectively. The input parameters are m_N (the mass of Nucleon), E_{lab} (the collision energy in lab frame) and \hat{s} (the collision energy at the parton level). The minimum energy for making a black hole (sphaleron) is controlled by $x_{\text{min}} = \text{Min}[\hat{s}/(2m_N E_{\text{lab}})]$. It is noted that if we set the unknown parameter of the sphaleron cross section $p \sim \mathcal{O}(1)$, the values of cross sections for sphaleron and black hole are numerically close to each other with $M_D \sim \mathcal{O}(1)$ TeV. Even though the production cross section for black holes eventually overtakes the sphaleron production, the luminosity of UHE cosmic ray becomes smaller at higher energies therefore the total event rates stay similar for the two different cases.

In Fig. 1, we show the relative sizes of the standard model NC/CC cross sections [51] and the expected cross sections from sphaleron and black hole with various pa-

parameter choices. We use NNPDF 3.0 [52] as the parton distribution function in the evaluation for CC/NC, sphaleron [43], and black hole production processes. We find that the sphaleron and black hole interactions will become increasingly important at higher energies as we expected: at low energies below 10^{6-7} GeV the standard model CC/NC neutrino-nucleon deep-inelastic scattering (DIS) dominates over other interactions as depicted by orange and brown lines. In a narrow resonance region at the W -boson threshold at $E_\nu = m_W^2/2m_e \simeq 6.3$ PeV, the W production process, $\bar{\nu}_e e^- \rightarrow W^-$, dominates as depicted by the green, mountain shape line (Glashow resonance). Above $\mathcal{O}(100)$ PeV, the new high multiplicity events, induced by electroweak sphaleron and black hole, become important and eventually dominate over the standard model CC/NC interactions.³ We depict the sphaleron events and black events with the parameters: $E_{\text{Sph}} = 8 - 10$ TeV for sphaleron (purple band) and $M_D = 1 - 2$ TeV with fixed $x_{\text{min}} \equiv M_{\text{min}}/M_D = 5$ for black hole. We take $M_D = 1$ TeV, $M_{\text{min}} = 5$ TeV (red band) and $M_D = 2$ TeV, $M_{\text{min}} = 10$ TeV (blue band) as our benchmark parameter choices. The bands for black hole are for various numbers of extra dimensions $2 \leq n \leq 6$ from bottom ($n = 2$) to top ($n = 6$). Finally the observational results for neutrino-nucleon cross section are depicted by black dots with error bars, which are from the 6-years IceCube data. In particular, we take the High Energy Starting Events (HESE) [53, 54], whose starting points of cascade or track are located inside the IceCube detector.

The proton-proton and proton-air cross sections are large and the QCD showers are dominant in low X_0 region. However, we show that the QCD background can be greatly reduced even below the new physics level by imposing a cut in high X_0^{cut} . The details are discussed later in Section A. After the cut, we take the sphaleron-induced and black hole air-showers with neutrino-nucleon collision as our signals, and CC/NC with neutrino-nucleon collision as our backgrounds.

III. EVENT RATES

As the fluxes of diffuse gamma rays and the GZK neutrino are correlated, the flux of GZK neutrinos can be determined from the diffuse gamma ray data taken e.g. by Fermi-LAT [55]. In Fig. 2, we collect the UHE neutrino fluxes obtained from various observational sources in the range of the energy, $E_{\text{sh}} \subset (10^8, 10^{10})$ GeV [10, 11]. In

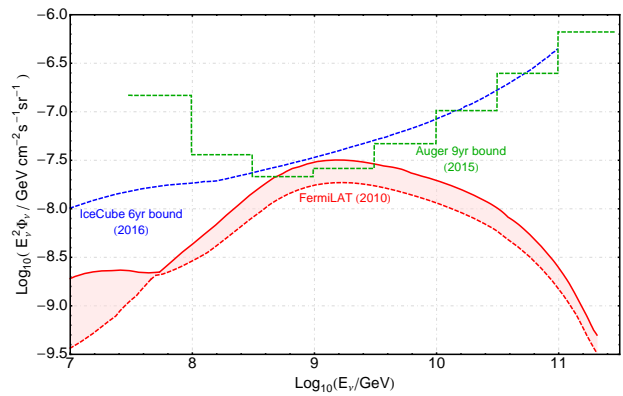


FIG. 2: [$E_\nu^2 \Phi_\nu$, GZK neutrino fluxes] Expected GZK neutrino fluxes and current experimental bounds. Expected GZK neutrino fluxes from the diffuse gamma-ray observation of Fermi-LAT [55] with the different crossover energies between $E_{\text{min}} = 10^{17.5} - 10^{19}$ eV (red band) and the current experimental bounds from IceCube [10, 11] (blue, dashed line) and Pierre Auger [13] (green, dashed line).

particular, we show the upper bounds on the fluxes obtained from ‘direct measurements’ from IceCube (2008-2014) [11] and Pierre Auger (2004-2013) [13]. We also show the flux obtained from ‘indirect measurement’ of Fermi-LAT gamma ray data [55] with different minimum energies of extragalactic cosmic rays involved in the photopion production.

It is clear from the figure, $E_{\text{sh}} \simeq (1 - 5) \times 10^9$ GeV regime for sphaleron is pretty close to the bounds from IceCube (2008-2014) and also Pierre Auger (2004-2013). However, black hole bound is still far below expected upper bound. Thus, we still need a significant upgrade of existing experiments to improve the situation.

IV. FEATURES OF NEW PHYSICS EVENTS

In this section, we describe some evident features of new physics events based on the symmetry principles and the quantum nature of Hawking radiation, which eventually provide useful guidelines to single out the new physics events from the background events.

A. Signals from Sphaleron: $(B - L)$ symmetry

For sphaleron, due to the symmetries of baryon number and lepton number, $\Delta(B - L) = 0$ and $\Delta(B + L) = 3n$ with an integer number n , the particle contents of the sphaleron process in the final state are almost uniquely determined. For instance, $\nu_e - N$ collision generates $(10 \text{ fermions}) + (n_B \text{ bosons})$ particles satisfying $\Delta B = \Delta L = -3$. The number of bosons (n_B bosons) is the sum of the number of gauge bosons ($n_W + n_Z$) and the

³ CC/NC interaction cross section has dominant contributions at small parton fraction as $x \lesssim 10^{-4}$ and cross section increase as $\sigma \sim E^\delta$ where the parton distribution fitted $xf_q(x) \sim x^{-\delta}$. In contrast, new physics (black hole or sphaleron) cross sections come from only large x region as $x \gtrsim x_{\text{min}} = E_{\text{min}}^2/2m_N E_\nu \gtrsim 10^{-4}$.

number of Higgs bosons (n_H).

More precisely, if up-type quark is in the initial nucleon N , the final state is

$$N(u) + \nu_e \rightarrow L + Q + n_W W + n_Z Z + n_H H \quad (4)$$

where L (Q) stands for the primary leptons (quarks), respectively. For example, $L = \mu^+ + \bar{\nu}_\tau$ and $Q = \bar{t} + 2\bar{b} + 2\bar{c} + \bar{s} + \bar{u} + \bar{d}$ is one of the possible minimal choices satisfying $L = 1$ to $L = -2$ and $B = 1/3$ to $B = -8/3$, respectively. In general, there are 2 antileptons ($L = -2$) and 8 antiquarks ($B = -8/3$) in a final state with possible addition of electroweak bosons. The secondary leptons from the decay of primary (heavy) quarks and gauge bosons are distinguishable as they are less energetic compared to the primary leptons.

Taking all the properties discussed above, we summarize the rules for the signal configuration:

- total $SU(2)_L$ isospin is conserved,
- $SU(3)$ color is conserved and the total color is singlet if initial and final states are considered all together,
- $\Delta B_i = \Delta L_j = \Delta N_{CS}$ for each families. ($i, j = 1, 2, 3$)
- total $U(1)_{EM}$ and $B - L$ charge are conserved.

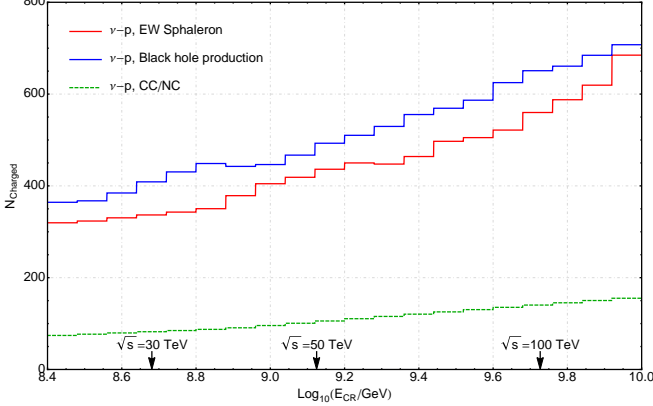


FIG. 3: [Charged particle multiplicity $N_{\text{Charged}} (\simeq N_{\pi^\pm}^{(0)})$]. The average number of charged particles after the primary hard interactions of neutrino-proton collision with CC/NC (green dashed line), EW sphaleron (red solid line) and microscopic black holes productions (blue solid line).

Typically, the final state of the sphaleron-induced process consists of $\mathcal{O}(10)$ hadronic jets and a few additional leptons in high energy domain and each particle carries an energy of about $E \approx M/n_{\text{primary}}$, where M is the new physics scale and n_{primary} is the number of primary decay products. The high multiplicity of hadronic components leads to lower individual pion's

energy $E_\pi \approx E_{\text{CR}}/(N_{\pi^\pm} + N_{\pi^0})$, thus the amount of energy loss is relatively smaller before reaching the critical energy, $E_{\text{crit}} = (1 - 10)$ GeV [56]. In Fig. 3 we show the number of charged particles (charged particle multiplicity, $N_{\text{Charged}} \simeq N_{\pi^\pm}^{(0)}$) from the different origins. The new physics induced air-showers have larger N_{Charged} . We used hadronic interaction models, QGSJET II-04 [57] and EPOS LHC [58] for calculation.

Below the critical energy, the charged pion's decay length, $\gamma c\tau_{\pi^\pm}$, becomes short in comparison to the interaction depth $\lambda_\pi \simeq 120 \text{ g cm}^{-2}$ of the atmosphere. In this stage, the charged pions decay mainly via $\pi^+ \rightarrow \mu^+ \nu_\mu$ before they interact with nuclei in air molecules. To some extent, the high multiplicity processes of new physics are similar to the processes due to heavy nuclei in the sense of the superposition model [59]. The extensive air shower from a heavy nuclei of the atomic mass A_{CR} with primary energy E_{CR} can be considered as a parallel copy of A_{CR} proton air-showers, and each of the proton carries the primary energy of about $E_{\text{CR}}/A_{\text{CR}}$. It is important to note that the number of muons included in the air shower at the observation level h_{obs} scales as $N_\mu \propto (A_{\text{CR}})^{1-\beta}$ [56] where $\beta = \ln \frac{N_{\pi^\pm}}{\frac{3}{2}N_{\pi^\pm}} = 0.85$ and $(A_{\text{CR}})^{1-\beta} \simeq 1.8$ for the iron nuclei, i.e. $A_{\text{CR}} = 56$.

As a summary, the main features of air-showers from the different origins are collectively shown in Fig. 4: the schematic picture of each air-shower event from different primary interactions and cosmic ray particles.

B. New Physics air-shower features at ground arrays

In addition to the high multiplicity of energetic hadronic components ($n_j \gtrsim 10$) with associated leptons, we also notice distinguishable features of the new physics events by performing realistic simulation of the air-shower events. The simulation is carried out aiming to see the new physics effects in the energy range $10^{15} \text{ eV} - 10^{20} \text{ eV}$ or collision energy of $\sqrt{s} = 10 - 300 \text{ TeV}$. As a benchmark, we set $E_{\text{Sph}} = 9.0 \text{ TeV}$ for electroweak sphaleron-induced events. In particular, we consider minimal signals without additional W -boson attached. From the events from the microscopic black-holes, we set $M_D = 1 - 2 \text{ TeV}$ and $M_{\text{min}} = 5M_D$, which is complementary to the LHC searches [60, 61]. Several MC tools are used for generating the extensive air-shower events: BlackMax [62] for the parton level black hole production and PYTHIA8 [63] for primary parton shower and hadronization. Finally CORSIKA [64] is used for extensive air-shower cascade where GHEISHA at low energies and QGSJET II-04 [57] (or EPOS LHC [58]) at high energies are attached for hadronic interactions in air-shower cascade simulations. A particularly useful quantity is the atmospheric slant interaction depth, $X(h)$, which is defined as the integrated density of atmosphere along the

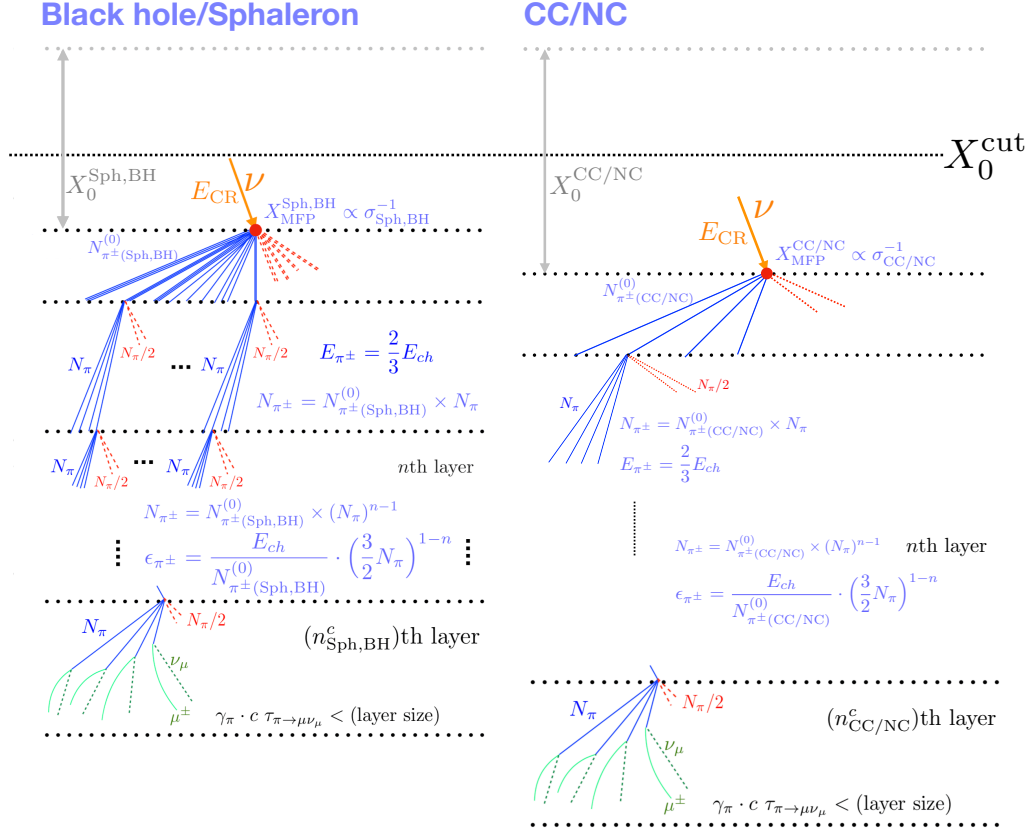


FIG. 4: [Schematic view of typical extensive air showers for two cases of primary hard interactions between neutrino and nucleon.] Left: EW sphaleron or black hole productions with a primary neutrino and a target nucleon. Right: CC/NC interactions with a primary neutrino and a target nucleon. Note that QCD backgrounds are removed by X_0 cut. Initial charged pion multiplicity $N_{\pi^\pm}^{(0)}(\text{Sph,BH})$, and $N_{\pi^\pm}^{(0)}(\text{CC/NC})$ are shown in Fig. 3.

path of air-shower,

$$X(h) \equiv \int_h^\infty dh' \rho_{\text{atm}}(h') \quad (5)$$

where $\rho_{\text{atm}}(h)$ is the density of the atmosphere at height h .

We mainly focus on the observables listed below.

- X_0 (Fig. 7): The first interaction point of air-showers, defined as

$$X_0 \equiv \int_{h_{\text{inj}}}^\infty dh' \rho_{\text{atm}}(h') \quad (6)$$

where h_{inj} is the height of the starting point (or injection point) of the air-shower induced by the collision of the UHE cosmic ray particle and the nucleon in the atmosphere. The typical air-shower events induced by the standard QCD interactions have a relatively steep distribution but the new physics interactions with a smaller cross section, $\sigma_{\text{NP}} \ll \sigma_{\text{QCD}}$, induce much broader distribution in

X_0 (See Fig. 7) as the probability distribution of the interaction point is given as

$$P(X_0) \propto \exp(-\sigma_{\text{int}} N_A A_{\text{atm}}^{-1} X_0) \quad (7)$$

where σ_{int} is the cross section of primary interaction and $A_{\text{atm}} = 14$ is the atomic mass of the atmosphere.

- $\Delta X (\equiv X_{\text{max}} - X_0)$ (Fig. 5): ΔX is the difference between the interaction depth position of the maximum charged particle multiplicity, X_{max} , and the first interaction depth. It is highly sensitive to the types of the relevant interactions. ΔX is observable at 24 fluorescence detector (FD) telescopes in the Auger observatories by measuring fluorescence light emitted from excited atmospheric (nitrogen) molecules in the range of 300 – 430 nm [65]. In particular, we focus on $\Delta X \equiv X_{\text{max}} - X_0$, the difference between maximum position and the initial position of showers.

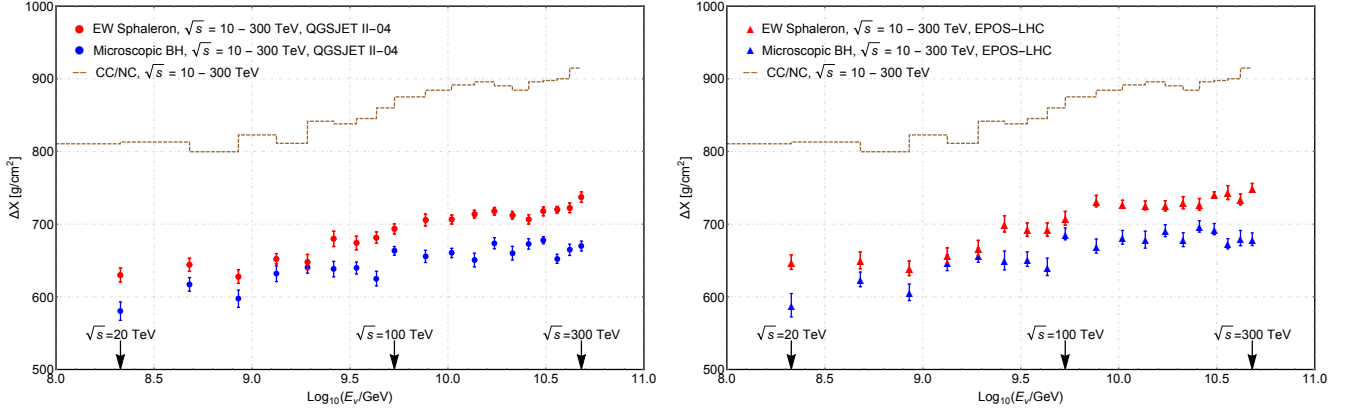


FIG. 5: [The Monte Carlo simulation of expectations of ΔX for EW sphaleron (red dot), black hole (blue), and CC/NC (brown dashed line) in $E_{CR} = 10^8 - 10^{11}$ GeV.] Note that circles (in the left panel) are the result with QGSJET II-04 [57] and triangles (in the right panel) are with EPOS-LHC [58] in its extensive shower event generation. ΔX values for CC/NC showers are also shown for comparison.

In Fig. 5, we depict the Monte Carlo simulation result of ΔX for EW sphaleron (left, red dots with error bars) and black hole (right, blue dots with error bars) in $E_{CR} = 10^8 - 10^{11}$ GeV. All error bars indicate the statistical error of the mean value, which is root-mean-square divided by square-root of the number of entries in each energy bin. Fig. 5 indicates ΔX values for new physics showers and ΔX for ordinary CC/NC showers are shown in comparison.⁴ We can easily notice that the sphaleron and black hole induced air-showers have smaller $\Delta X (= X_{\max} - X_0)$ values compared to CC/NC air-showers. Our results are consistent with earlier simulation for sphaleron-induced [66] and black hole-induced [67] air-showers. The new physics induced air-showers by sphaleron and black hole have broader distributions in their injection positions h_{inj} . (See Appendix. C for more details).

Imposing X_0^{cut} (Fig. 7) and ΔX^{cut} (Fig. 5), our selection criterion for signal is given by

- i) $X_0 > X_0^{\text{cut}} = 1200 \text{ g/cm}^2$, (8)
- ii) $\Delta X < \Delta X^{\text{cut}} \simeq 50 \text{ Log}_{10}(E_{CR}/\text{GeV}) + 260 \text{ g/cm}^2$. (9)

One can expect new physics showers from signal yields under these cuts. Huge QCD backgrounds can be removed by X_0^{cut} , and new physics showers can be distinguished from remaining CC/NC shower backgrounds by considering ΔX^{cut} . If we consider the view in Fig. 4, we estimate the maximum position as follows [68]:

$$X_{\max} \simeq X_0 + X_{\text{MFP}}^{\pi p} \ln \left(\frac{E_{CR}}{N_{\pi^\pm}^{(0)} \cdot E_{\text{crit.}}} \right) \quad (10)$$

⁴ $X_{\max} (= X_0 + \Delta X)$ distribution for new physics shower will be much broader since X_0 are almost uniformly distributed.

where $N_{\pi^\pm}^{(0)}$ is the number of charged pions produced in the first hard interactions indicated in Fig. 3 for each interactions, and $X_{\text{MFP}}^{\pi p} = 120 \text{ g/cm}^2$ is the mean-free-depth of pions in the atmosphere. $E_{\text{crit.}}$ is the minimum energy of charged pions satisfying $\gamma_\pi c \tau_{\pi^\pm} < (\text{layer size})$, in order to make the pions reinteract with nucleons in air molecules before they decay into muons and neutrinos. As a result, the difference $X_{\max}^{\text{CC/NC}} - X_{\max}^{\text{NP}}$ is given by

$$X_{\max}^{\text{CC/NC}} - X_{\max}^{\text{Sph,BH}} \simeq \ln \left(\frac{N_{\pi^\pm}^{(0)}(\text{Sph,BH})}{N_{\pi^\pm}^{(0)}(\text{CC/NC})} \right) \quad (11)$$

Clearly, we notice that the value $\ln \left(\frac{E_{CR}}{N_{\pi^\pm}^{(0)} \cdot E_{\text{crit.}}} \right)$ corresponds to the number of layers in Fig. 4.

C. The muon number in the UHECR events

Finally, in this section, we address the anomalous result reported by the Pierre Auger collaboration with their 9-years data [37, 38] and see the potential account from the new physics effects. The 9-years (2004-2013) Pierre Auger Observatory data set contains many UHE cosmic ray air-shower events, including 29,722 ‘highly inclined events’ with the event selection criteria:

- $62^\circ < \theta_{\text{zenith}} < 80^\circ$ with $\theta_{\text{zenith}}^{\text{avg.}} = 67^\circ$,
- $E_{\mu^\pm} > 0.3 \text{ GeV}$
- $E_{CR} \geq 5 \times 10^{18} \text{ eV}$

Among these 29,722 events, there are 174 events indicate the deficit of muons in the Monte Carlo simulations. These highly inclined shower events have more muons than the expected number of muons predicted by the hadronic models. Importantly, the muon number is detectable via SD/FD hybrid detection [37, 38]. Specifically, $R_\mu = N_\mu/N_{\mu,19}$ parameter is used to define the

normalized muon number in each extensive air shower event: the total number of muons in each event divided by the reference value of the muon number. We take the reference value $N_{\mu,19} = 2.68 \times 10^7$ at $\theta_{\text{zenith}} = 67^\circ$ from Ref. [37], which is obtained from the MC simulation at $E_{\text{CR}} = 10^{19}$ eV. We take these events seriously since the similar muon issues are also found in TA 7-years (2008-2015) data set [39]. The deficit in interaction models mainly appear in highly inclined and highest energies air-showers [69]. To account the muon issue in air-shower events, several approaches have been proposed even though no thorough explanation has been given, including the revision of hadronic interaction models at high energy collisions in $\sqrt{s} = 110 - 170$ TeV range [70] as well as new physics contributions [71, 72].

We check if the new physics interactions due to sphaleron or black hole improves the situation. The results are shown in Fig. 6. The new physics interactions indeed provide some enhancement compared with the QCD events (proton, iron with different modelings) at high energies, $E > 10^{9.5}$ GeV. However, when the muon number is averaged over the energy ranges, $R_{\mu}^{\text{avg}}(E_{\text{CR}})$, the new physics interactions do not provide any significant enhancement except for the very deep injection from $h_{\text{inj}} \lesssim 5.0$ km (or equivalently, $X_0 \gtrsim 1400$ g/cm²), which is not very likely for the new physics. In conclusion, the new physics interactions -by sphaleron and black hole- do not seem to explain the muon deficit in the air showers generated by the hadronic interaction models.

As we mention in Appendix A, the muon number measurement for highly-inclined air-showers still can be informative for new physics search after imposing the X_0 cut.

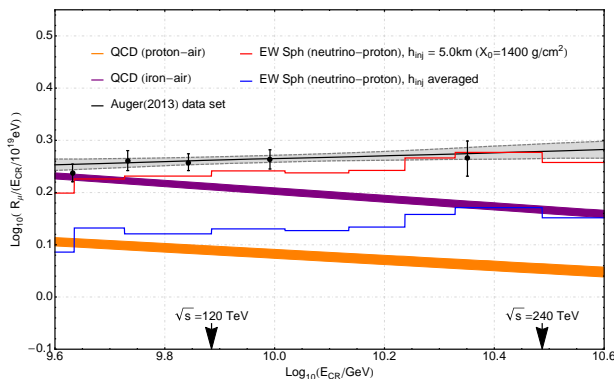


FIG. 6: The total number of muons in highly-inclined air-showers of 9-years Auger data [37] and the expected muon numbers for sphaleron-induced air-showers for a fixed initial injection height $h_{\text{inj}} = 5.0$ km of extensive air showers (red solid line). The depth-averaged muon number is also shown (blue solid line).

V. CONCLUSION

Targeting potential new physics located at $\mathcal{O}(10)$ TeV, we studied generic search strategies at the air-shower detector array experiments such as Telescope Array Experiment and Pierre-Auger Observatory, where the collisions of UHECRs and nucleons in the atmosphere are observed. Comparing the signal events with conventional QCD events, we found that our target events have larger multiplicities and thus have characteristic features in showering processes: broader X_0 , larger N_{Charged} at higher energies, and also distinguishable numbers of electromagnetic, muonic and hadronic components. The features are highlighted in the schematic figure in Fig. 4. Finally, we also studied potential implication of new physics interactions to the ‘muon deficit in models’ seen in Auger and TA data. Some details of our analysis are presented in the appendices.

When the improved determination of the mass composition [73] is achieved and the origin of UHECR is better clarified in the future [74], the cosmic ray air-shower events from the high-multiplicity processes can be better probed based on our analysis. We expect the future air-shower array experiments such as TA \times 4 [75], FAST [76], GRAND [77] POEMMA [78], and AugerPrime [79] will reveal the nature of physics at TeV and beyond.

ACKNOWLEDGMENTS

This work was supported by the National Research Foundation of Korea (NRF) grants funded by the Korean government (MSIP)(NRF-2018R1A4A1025334) and (NRF-2019R1A2C1089334).

Appendix A: Cutting the background events

In general, the QCD background events from the collision of UHECR proton/nucleon and proton/nucleon in the atmosphere are dominant sources of shower events observed at a ground based experiment. However, imposing an aggressive cut at a large X_0 greatly reduces the background as observed in Ref. [33]. Taking the short mean-free-depth $\lambda_{\text{QCD}} \sim 80$ g/cm² for the QCD event, we found that the cut $X_0^{\text{cut}} \gtrsim 1200$ g/cm² removes almost all QCD backgrounds. The neutrino events, by new physics (black hole, sphaleron) or CC/NC, on the other hand, have longer mean-free-depth and the event distribution is uniform thus remains relatively large as clearly seen in Fig. 7.

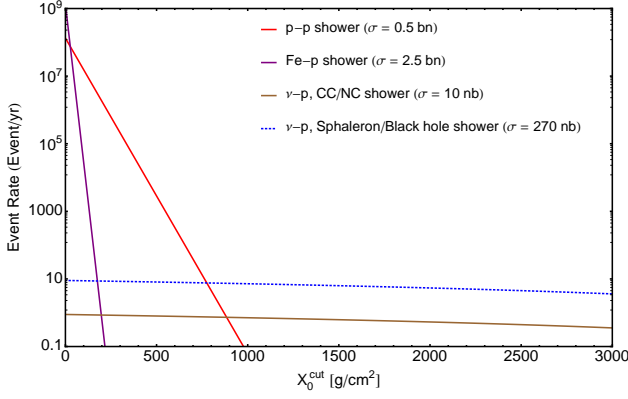


FIG. 7: **Event rate on ground detector array after X_0 cut.** Expected number of events per year on Auger after injection point cut X_0^{cut} for primary particle energy $10^8 \text{ GeV} < E_{\text{CR}} < 10^{11} \text{ GeV}$. New physics event is neutrino-nucleon collision induced by electroweak sphaleron (Eq. 1 with $p = 1.0$). Total event numbers are obtained for the maximum slant depth $X = 5000 \text{ g/cm}^2$ which corresponds to $\theta_{\text{zenith}} = 80^\circ$. We use (C2) for X_0 distribution with σ_{int} as each cross sections indicated in the figure.

Appendix B: Event rate in the air-shower detector array

1. CC/NC neutrino-induced deep inclined air-shower event

The CC/NC neutrino-induced, nearly horizontal deep air-shower event rates on the Pierre Auger, for each shower origin, are [51]

- NC shower for all 3 flavors $\nu_{l=e,\mu,\tau}$ and $\bar{\nu}_{l=e,\mu,\tau}$. ($\nu_l q \rightarrow \nu_l q^*$)

$$\frac{dN_{\nu}^{\text{NC}}}{dt} = \rho_{\text{Air}} N_A \sum_{l=e,\mu,\tau} \int_{E_{\text{min}}}^{\infty} dE_{\text{sh}} \frac{d\phi_{\nu_l}(E_{\nu})}{dE_{\nu}} \times \int_{y_{\text{min}}}^{y_{\text{max}}} dy \frac{d\sigma_{\nu_l}^{\text{NC}}(E_{\nu}, y)}{dy} \mathcal{A}(E_{\text{sh}}) \quad (\text{B1})$$

where $E_{\text{sh}} = yE_{\nu} = E_{\nu} - E'_{\nu}$ is the total hadronic shower energy.

- CC shower for ν_e and $\bar{\nu}_e$. ($\nu_e q \rightarrow e q'$)

$$\frac{dN_{\nu_e}^{\text{CC}}}{dt} = \rho_{\text{Air}} N_A \int_{E_{\text{min}}}^{\infty} dE_{\text{sh}} \frac{d\phi_{\nu_e}(E_{\nu})}{dE_{\nu}} \times \int_0^1 dy \frac{d\sigma_{\nu_e}^{\text{CC}}(E_{\nu}, y)}{dy} \Theta(E_{\text{max}} - E_{\nu}) \mathcal{A}(E_{\text{sh}}) \quad (\text{B2})$$

where $yE_{\nu} = E_{\nu} - E_e$ and E_e is the hadronic shower and EM shower energy, respectively. The total shower energy is $E_{\text{sh}} = E_{\nu}$.

- CC shower for ν_{τ} and $\bar{\nu}_{\tau}$ with hadronically decaying τ ($\nu_{\tau} q \rightarrow \tau q'$, and $\tau \rightarrow \nu_{\tau} q'' \bar{q}'''$)

$$\begin{aligned} \frac{dN_{\nu_{\tau}}^{\text{CC-had}}}{dt} &= \rho_{\text{Air}} N_A \int_{E_{\text{min}}}^{\infty} dE_{\text{sh}} \frac{d\phi_{\nu_{\tau}}(E_{\nu})}{dE_{\nu}} \\ &\times \int_0^1 dy \frac{d\sigma_{\nu_{\tau}}^{\text{CC}}(E_{\nu}, y)}{dy} \int_0^1 dz \frac{dn(\tau \rightarrow \text{had})}{dz} \\ &\times \Theta(E_{\nu}(y + (1-y)(1-z)) - E_{\text{min}}) \\ &\times \Theta(E_{\text{max}} - E_{\nu}(y + (1-y)(1-z))) \\ &\times \text{Br}(\tau \rightarrow \text{hadrons}) \times \mathcal{A}(E_{\text{sh}}) \quad (\text{B3}) \end{aligned}$$

where $yE_{\nu} = E_{\nu} - E_{\tau}$ is the deposited energy, and $z = E'_{\nu}/E_{\tau}$ is the fraction of invisible (neutrino) energy from tau decays and total shower energy is the sum of hadronic energy of the broken nucleon yE_{ν} and hadronic energy from tau decays $(1-y)(1-z)E_{\nu}$.

- CC shower for ν_{τ} and $\bar{\nu}_{\tau}$ with electronically decaying τ ($\nu_{\tau} q \rightarrow \tau q'$, and $\tau \rightarrow \nu_{\tau} \bar{\nu}_e e$)

$$\begin{aligned} \frac{dN_{\nu_{\tau}}^{\text{CC-em}}}{dt} &= \rho_{\text{Air}} N_A \int_{E_{\text{min}}}^{\infty} dE_{\text{sh}} \frac{d\phi_{\nu_{\tau}}(E_{\nu})}{dE_{\nu}} \\ &\times \int_0^1 dy \frac{d\sigma_{\nu_{\tau}}^{\text{CC}}(E_{\nu}, y)}{dy} \int_0^1 dz \frac{dn(\tau \rightarrow \nu_{\tau} \bar{\nu}_e e)}{dz} \\ &\times \Theta(E_{\nu}(y + (1-y)z) - E_{\text{min}}) \\ &\times \Theta(E_{\text{max}} - E_{\nu}(y + (1-y)z)) \\ &\times \text{Br}(\tau \rightarrow \nu_{\tau} \bar{\nu}_e e) \times \mathcal{A}(E_{\text{sh}}) \quad (\text{B4}) \end{aligned}$$

where $yE_{\nu} = E_{\nu} - E_{\tau}$ is the deposited energy again, and $z = E_e/E_{\tau}$ is the fraction of EM shower energy from tau decays and total shower energy is the sum of hadronic energy of broken nucleon yE_{ν} and tau EM shower energy $(1-y)zE_{\nu}$.

- CC shower for ν_{μ} and $\bar{\nu}_{\mu}$. ($\nu_{\mu} q \rightarrow \mu q'$)

$$\frac{dN_{\nu_{\mu}}^{\text{CC-had}}}{dt} = \rho_{\text{Air}} N_A \int_{E_{\text{min}}}^{\infty} dE_{\text{sh}} \frac{d\phi_{\nu_{\mu}}(E_{\nu})}{dE_{\nu}} \times \int_{y_{\text{min}}}^{y_{\text{max}}} dy \frac{d\sigma_{\nu_{\mu}}^{\text{CC}}(E_{\nu}, y)}{dy} \mathcal{A}(E_{\text{sh}}) \quad (\text{B5})$$

where $E_{\text{sh}} = yE_{\nu} = E_{\nu} - E_{\mu}$ is the total shower energy.

- CC shower for ν_{τ} and $\bar{\nu}_{\tau}$ with muonically decaying τ ($\nu_{\tau} q \rightarrow \tau q'$, and $\tau \rightarrow \nu_{\tau} \bar{\nu}_{\mu} \mu$)

$$\begin{aligned} \frac{dN_{\nu_{\tau}}^{\text{CC-had}}}{dt} &= \rho_{\text{Air}} N_A \int_{E_{\text{min}}}^{\infty} dE_{\text{sh}} \frac{d\phi_{\nu_{\tau}}(E_{\nu})}{dE_{\nu}} \\ &\times \text{Br}(\tau \rightarrow \nu_{\tau} \bar{\nu}_{\mu} \mu) \\ &\times \int_{y_{\text{min}}}^{y_{\text{max}}} dy \frac{d\sigma_{\nu_{\tau}}^{\text{CC}}(E_{\nu}, y)}{dy} \mathcal{A}(E_{\text{sh}}) \quad (\text{B6}) \end{aligned}$$

where $E_{\text{sh}} = yE_\nu = E_\nu - E_\tau$ is the total shower energy, again.

For the detailed evaluation, we need several quantities defining the detector size, the strength of each interaction and the flux of neutrinos from various sources such as

- $\mathcal{A}(E_{\text{sh}})$ is the energy-dependent effective array acceptance [80, 81] for all interactions (same for all flavors $\nu_{l=e,\mu,\tau}$). Basically, the Pierre Auger detector array is sensitive above $\mathcal{O}(100)$ PeV, in which GZK neutrinos are dominant.
- $d\sigma_{\nu_l}^{CC,NC}/dy$ is the differential CC and NC neutrino (ν_l)-nucleon (N) cross section in the SM [51] respectively, and the total cross sections are

$$\sigma_{\nu_l}^{CC}(E_\nu) = \frac{2G_f^2 M_N E_\nu}{\pi} \int_0^1 dy \int_0^1 dx \left(\frac{M_W^2}{Q^2 + M_W^2} \right)^2 \times \sum_q \left[x f_q(x, Q^2) + x f_{\bar{q}}(x, Q^2)(1-y)^2 \right], \quad (\text{B7})$$

$$\sigma_{\nu_l}^{NC}(E_\nu) = \frac{G_F^2 M_N E_\nu}{2\pi} \int_0^1 dy \int_0^1 dx \left(\frac{M_Z^2}{Q^2 + M_Z^2} \right)^2 \times \sum_q \left[x f_{q^0}(x, Q^2) + x f_{\bar{q}^0}(x, Q^2)(1-y)^2 \right], \quad (\text{B8})$$

where x is the parton fraction in the nucleon, and y is the fraction of deposited energy. $f_q(x, Q^2)$ and $f_{\bar{q}}(x, Q^2)$ are also defined in [51].

- The energy spectrums dn/dz in electronically [82] and hadronically [83] decaying τ and the branching ratio in the τ decay.
- There are neutrinos due to the interaction between high-energy cosmic rays and Earth atmosphere nuclei [84] and the neutrinos of the astrophysical origin, such as highly-accelerated hadrons in supernovae remnants, active galactic nuclei (AGN), gamma-ray bursts (GRBs), and shocks in star formation regions of galaxies [85].
- Above $\mathcal{O}(100)$ PeV, the UHE neutrinos are produced by the interaction between the UHE cosmic rays (mainly protons, and small fractions of other heavy nuclei) above $\mathcal{O}(10^9)$ GeV and the CMB photons [86, 87], by the following channels: $p + \gamma_{\text{bkg.}} \rightarrow \pi^+ + n$, $\pi^+ \rightarrow \mu^+ + \nu_\mu$ and $p + \gamma_{\text{bkg.}} \rightarrow \pi^0 + p$, $\pi^0 \rightarrow \gamma + \gamma$. This generation of pions is also denoted as the photo-pion production. The cross section for pion production has a resonance peak

at the $\Lambda^+(1232)$ resonance [88]. These UHE neutrinos from the GZK mechanism are expected from the observations of the UHE cosmic rays by the air-shower detector arrays [1, 2] and the observations of diffuse photons by the gamma-ray telescopes [55], although there is no direct observation of the GZK neutrinos by the neutrino telescopes yet [10, 11].

The UHE neutrinos can produce nearly horizontal and deep air-showers, which correspond to $X \sim 13,000$ g/cm² [12]. For typical flux values and CC/NC interactions, we expect $\sim (0.9 - 2.9)$ events/yr with typical choices of the acceptance values and the GZK neutrino flux models, although no neutrino-induced event candidates have been found yet [80], which provides the bound on the GZK neutrino flux.

2. New physics air-shower event

The event rate in the ground air-shower detector array is given by

$$\frac{dN}{dt} = N_A \rho_{\text{air}} \int_{E_{\text{th}}}^{E_{\text{max}}} dE_{\text{sh}} \int_0^1 dy \times \frac{d\phi_{\nu_l}(E_\nu)}{dE_\nu} \frac{d\sigma_{\nu_l X}(E_\nu, y)}{dy} \mathcal{A}(E_{\text{sh}}). \quad (\text{B9})$$

where $\mathcal{A}(E_{\text{sh}})$ is the air-shower energy-dependent acceptance of the entire detector array. We adopt the values in [80, 81] for Auger.

Appendix C: Mean-Free-Path weighted muon number

The mean-free-path averaged muon number, which is given by

$$R_\mu^{\text{avg.}}(E_{\text{CR}}) = \int_0^{X_{\text{obs.}}} dX_0 P(X_0, \sigma_{\text{int}}(E_\nu)) R_\mu(X_0, E_\nu) \quad (\text{C1})$$

where

$$P(X_0, \sigma_{\text{int}}(E_\nu)) = \frac{1}{X_{\text{MFP}}(\sigma_{\text{int}}(E_\nu))} \times \exp\left(-X_0/X_{\text{MFP}}(\sigma_{\text{int}}(E_\nu))\right) \quad (\text{C2})$$

and $X_{\text{MFP}}(\sigma_{\text{int}}) = A_{\text{atm}} \cdot N_A^{-1} \cdot \sigma_{\text{int}}^{-1}(E_\nu)$ is the mean-free-depth. A_{atm} is the atomic mass of the atmosphere. Because the cross section for new physics σ_{int} is small enough for our parameter choices, $P(X_0, \sigma_{\text{int}})$ is almost constant and the air-showers can occur everywhere with almost uniform distribution.

-
- [1] PIERRE AUGER collaboration, I. Valino, *The flux of ultra-high energy cosmic rays after ten years of operation of the Pierre Auger Observatory, PoS ICRC2015* (2016) 271.
- [2] TELESCOPE ARRAY collaboration, P. Tinyakov, *TA Anisotropy Summary, JPS Conf. Proc.* **19** (2018) 011019.
- [3] ICECUBE collaboration, M. G. Aartsen et al., *First observation of PeV-energy neutrinos with IceCube, Phys. Rev. Lett.* **111** (2013) 021103 [1304.5356].
- [4] P. Blasi, R. I. Epstein and A. V. Olinto, *Ultrahigh-energy cosmic rays from young neutron star winds, Astrophys. J.* **533** (2000) L123 [astro-ph/9912240].
- [5] F. Halzen and E. Zas, *Neutrino fluxes from active galaxies: A Model independent estimate, Astrophys. J.* **488** (1997) 669 [astro-ph/9702193].
- [6] E. Waxman, *Cosmological origin for cosmic rays above 10^{19} -eV, Astrophys. J.* **452** (1995) L1 [astro-ph/9508037].
- [7] M. Vietri, *On the acceleration of ultrahigh-energy cosmic rays in gamma-ray bursts, Astrophys. J.* **453** (1995) 883 [astro-ph/9506081].
- [8] D. S. Gorbunov, P. G. Tinyakov, I. I. Tkachev and S. V. Troitsky, *Testing the correlations between ultra-high-energy cosmic rays and BL Lac type objects with HiRes stereoscopic data, JETP Lett.* **80** (2004) 145 [astro-ph/0406654].
- [9] P. Bhattacharjee and G. Sigl, *Origin and propagation of extremely high-energy cosmic rays, Phys. Rept.* **327** (2000) 109 [astro-ph/9811011].
- [10] ICECUBE collaboration, M. G. Aartsen et al., *The IceCube Neutrino Observatory - Contributions to ICRC 2015 Part II: Atmospheric and Astrophysical Diffuse Neutrino Searches of All Flavors, in Proceedings, 34th International Cosmic Ray Conference (ICRC 2015): The Hague, The Netherlands, July 30-August 6, 2015, 1510.05223, https://inspirehep.net/record/1398539/files/arXiv:1510.05223.pdf* [1303.4603].
- [11] ICECUBE collaboration, A. Ishihara, *Extremely high energy neutrinos in six years of IceCube data, J. Phys. Conf. Ser.* **718** (2016) 062027.
- [12] PIERRE AUGER collaboration, P. Abreu et al., *Ultrahigh Energy Neutrinos at the Pierre Auger Observatory, Adv. High Energy Phys.* **2013** (2013) 708680 [1304.1630].
- [13] PIERRE AUGER collaboration, A. Aab et al., *Improved limit to the diffuse flux of ultrahigh energy neutrinos from the Pierre Auger Observatory, Phys. Rev.* **D91** (2015) 092008 [1504.05397].
- [14] TELESCOPE ARRAY collaboration, R. U. Abbasi et al., *Depth of Ultra High Energy Cosmic Ray Induced Air Shower Maxima Measured by the Telescope Array Black Rock and Long Ridge FADC Fluorescence Detectors and Surface Array in Hybrid Mode, Astrophys. J.* **858** (2018) 76 [1801.09784].
- [15] *Pierre Auger Observatory and Telescope Array: Joint Contributions to the 35th International Cosmic Ray Conference (ICRC 2017)*, 2018.
- [16] L. A. Anchordoqui, *Ultra-High-Energy Cosmic Rays, Phys. Rep.* **801** (2019) 1 [1807.09645].
- [17] N. S. Manton, *Topology in the Weinberg-Salam Theory, Phys. Rev.* **D28** (1983) 2019.
- [18] F. R. Klinkhamer and N. S. Manton, *A Saddle Point Solution in the Weinberg-Salam Theory, Phys. Rev.* **D30** (1984) 2212.
- [19] V. A. Kuzmin, V. A. Rubakov and M. E. Shaposhnikov, *On the Anomalous Electroweak Baryon Number Nonconservation in the Early Universe, Phys. Lett.* **155B** (1985) 36.
- [20] M. Fukugita and T. Yanagida, *Baryogenesis Without Grand Unification, Phys. Lett.* **B174** (1986) 45.
- [21] M. E. Shaposhnikov, *Baryon Asymmetry of the Universe in Standard Electroweak Theory, Nucl. Phys.* **B287** (1987) 757.
- [22] A. Ringwald, *Sphaleron and Level Crossing, Phys. Lett.* **B213** (1988) 61.
- [23] V. A. Rubakov and M. E. Shaposhnikov, *Electroweak baryon number nonconservation in the early universe and in high-energy collisions, Usp. Fiz. Nauk* **166** (1996) 493 [hep-ph/9603208].
- [24] A. Ringwald, *Electroweak instantons / sphalerons at VLHC?, Phys. Lett.* **B555** (2003) 227 [hep-ph/0212099].
- [25] S. Dimopoulos and G. L. Landsberg, *Black holes at the LHC, Phys. Rev. Lett.* **87** (2001) 161602 [hep-ph/0106295].
- [26] S. B. Giddings and S. D. Thomas, *High-energy colliders as black hole factories: The End of short distance physics, Phys. Rev.* **D65** (2002) 056010 [hep-ph/0106219].
- [27] S. C. Park, *Black holes and the LHC: A Review, Prog. Part. Nucl. Phys.* **67** (2012) 617 [1203.4683].
- [28] N. Arsene, L. I. Caramete, P. B. Denton and O. Micu, *Quantum Black Holes Effects on the Shape of Extensive Air Showers, Rom. Rep. Phys.* **69** (2017) 105 [1310.2205].
- [29] N. Arsene, X. Calmet, L. I. Caramete and O. Micu, *Back-to-Back Black Holes decay Signature at Neutrino Observatories, Astropart. Phys.* **54** (2014) 132 [1303.4603].
- [30] N. Arsene, R. Casadio and O. Micu, *Quantum production of black holes at colliders, Eur. Phys. J.* **C76** (2016) 384 [1606.07323].
- [31] T. Ježo, M. Klasen, F. Lyonnet, F. Montanet, I. Schienbein and M. Tartare, *Can new heavy gauge bosons be observed in ultra-high energy cosmic neutrino events?, Phys. Rev.* **D89** (2014) 077702 [1401.6012].
- [32] L. Anchordoqui and H. Goldberg, *Experimental signature for black hole production in neutrino air showers, Phys. Rev.* **D65** (2002) 047502 [hep-ph/0109242].
- [33] L. A. Anchordoqui, J. L. Feng, H. Goldberg and A. D. Shapere, *Black holes from cosmic rays: Probes of extra dimensions and new limits on TeV scale gravity, Phys. Rev.* **D65** (2002) 124027 [hep-ph/0112247].
- [34] A. Ringwald and H. Tu, *Collider versus cosmic ray sensitivity to black hole production, Phys. Lett.* **B525** (2002) 135 [hep-ph/0111042].
- [35] L. A. Anchordoqui, J. L. Feng, H. Goldberg and A. D. Shapere, *Updated limits on TeV scale gravity from absence of neutrino cosmic ray showers mediated by black holes, Phys. Rev.* **D68** (2003) 104025

- [hep-ph/0307228].
- [36] L. Anchordoqui, T. Han, D. Hooper and S. Sarkar, *Exotic neutrino interactions at the Pierre Auger Observatory*, *Astropart. Phys.* **25** (2006) 14 [[hep-ph/0508312](#)].
- [37] PIERRE AUGER collaboration, A. Aab et al., *Muons in air showers at the Pierre Auger Observatory: Mean number in highly inclined events*, *Phys. Rev.* **D91** (2015) 032003 [[1408.1421](#)].
- [38] PIERRE AUGER collaboration, A. Aab et al., *Muons in air showers at the Pierre Auger Observatory: Measurement of atmospheric production depth*, *Phys. Rev.* **D90** (2014) 012012 [[1407.5919](#)].
- [39] TELESCOPE ARRAY collaboration, R. U. Abbasi et al., *Study of muons from ultrahigh energy cosmic ray air showers measured with the Telescope Array experiment*, *Phys. Rev.* **D98** (2018) 022002 [[1804.03877](#)].
- [40] A. Ringwald, *High-Energy Breakdown of Perturbation Theory in the Electroweak Instanton Sector*, *Nucl. Phys.* **B330** (1990) 1.
- [41] D. A. Morris and A. Ringwald, *Cosmic ray signatures of multi - W processes*, *Astropart. Phys.* **2** (1994) 43 [[hep-ph/9308269](#)].
- [42] J. Ellis and K. Sakurai, *Search for Sphalerons in Proton-Proton Collisions*, *JHEP* **04** (2016) 086 [[1601.03654](#)].
- [43] J. Ellis, K. Sakurai and M. Spannowsky, *Search for Sphalerons: IceCube vs. LHC*, *JHEP* **05** (2016) 085 [[1603.06573](#)].
- [44] K. Funakubo, K. Fuyuto and E. Senaha, *Does a band structure affect sphaleron processes?*, [1612.05431](#).
- [45] S. H. H. Tye and S. S. C. Wong, *Baryon Number Violating Scatterings in Laboratories*, *Phys. Rev.* **D96** (2017) 093004 [[1710.07223](#)].
- [46] S. H. H. Tye and S. S. C. Wong, *Bloch Wave Function for the Periodic Sphaleron Potential and Unsuppressed Baryon and Lepton Number Violating Processes*, *Phys. Rev.* **D92** (2015) 045005 [[1505.03690](#)].
- [47] S. W. Hawking, *Black hole explosions*, *Nature* **248** (1974) 30.
- [48] S. W. Hawking, *Particle Creation by Black Holes*, *Commun. Math. Phys.* **43** (1975) 199.
- [49] S. C. Park and H. S. Song, *Production of spinning black holes at colliders*, *J. Korean Phys. Soc.* **43** (2003) 30 [[hep-ph/0111069](#)].
- [50] H. Yoshino and Y. Nambu, *Black hole formation in the grazing collision of high-energy particles*, *Phys. Rev.* **D67** (2003) 024009 [[gr-qc/0209003](#)].
- [51] R. Gandhi, C. Quigg, M. H. Reno and I. Sarcevic, *Neutrino interactions at ultrahigh-energies*, *Phys. Rev.* **D58** (1998) 093009 [[hep-ph/9807264](#)].
- [52] NNPDF collaboration, R. D. Ball et al., *Parton distributions for the LHC Run II*, *JHEP* **04** (2015) 040 [[1410.8849](#)].
- [53] ICECUBE collaboration, M. G. Aartsen et al., *Measurement of the multi-TeV neutrino cross section with IceCube using Earth absorption*, *Nature* (2017) [[1711.08119](#)].
- [54] M. Bustamante and A. Connolly, *Measurement of the Energy-Dependent Neutrino-Nucleon Cross Section Above 10 TeV Using IceCube Showers*, [1711.11043](#).
- [55] M. Ahlers, L. A. Anchordoqui, M. C. Gonzalez-Garcia, F. Halzen and S. Sarkar, *GZK Neutrinos after the Fermi-LAT Diffuse Photon Flux Measurement*, *Astropart. Phys.* **34** (2010) 106 [[1005.2620](#)].
- [56] J. Matthews, *A Heitler model of extensive air showers*, *Astropart. Phys.* **22** (2005) 387.
- [57] S. Ostapchenko, *Monte Carlo treatment of hadronic interactions in enhanced Pomeron scheme: I. QGSJET-II model*, *Phys. Rev.* **D83** (2011) 014018 [[1010.1869](#)].
- [58] T. Pierog, I. Karpenko, J. M. Katzy, E. Yatsenko and K. Werner, *EPOS LHC: Test of collective hadronization with data measured at the CERN Large Hadron Collider*, *Phys. Rev.* **C92** (2015) 034906 [[1306.0121](#)].
- [59] J. Engel, T. K. Gaisser, T. Stanev and P. Lipari, *Nucleus-nucleus collisions and interpretation of cosmic ray cascades*, *Phys. Rev.* **D46** (1992) 5013.
- [60] ATLAS collaboration, G. Aad et al., *Search for strong gravity in multijet final states produced in pp collisions at $\sqrt{s} = 13$ TeV using the ATLAS detector at the LHC*, *JHEP* **03** (2016) 026 [[1512.02586](#)].
- [61] ATLAS collaboration, M. Aaboud et al., *Search for TeV-scale gravity signatures in high-mass final states with leptons and jets with the ATLAS detector at $\sqrt{s} = 13$ TeV*, *Phys. Lett.* **B760** (2016) 520 [[1606.02265](#)].
- [62] D.-C. Dai, G. Starkman, D. Stojkovic, C. Issever, E. Rizvi and J. Tseng, *BlackMax: A black-hole event generator with rotation, recoil, split branes, and brane tension*, *Phys. Rev.* **D77** (2008) 076007 [[0711.3012](#)].
- [63] T. Sjostrand, S. Mrenna and P. Z. Skands, *A Brief Introduction to PYTHIA 8.1*, *Comput. Phys. Commun.* **178** (2008) 852 [[0710.3820](#)].
- [64] D. Heck, G. Schatz, J. Knapp, T. Thouw and J. Capdevielle, *CORSIKA: A Monte Carlo Code to Simulate Extensive Air Showers*, .
- [65] PIERRE AUGER collaboration, J. Abraham et al., *The Fluorescence Detector of the Pierre Auger Observatory*, *Nucl. Instrum. Meth.* **A620** (2010) 227 [[0907.4282](#)].
- [66] G. Brooijmans, P. Schichtel and M. Spannowsky, *Cosmic ray air showers from sphalerons*, *Phys. Lett.* **B761** (2016) 213 [[1602.00647](#)].
- [67] E.-J. Ahn and M. Cavaglia, *Simulations of black hole air showers in cosmic ray detectors*, *Phys. Rev.* **D73** (2006) 042002 [[hep-ph/0511159](#)].
- [68] S. Mollerach and E. Roulet, *Progress in high-energy cosmic ray physics*, *Prog. Part. Nucl. Phys.* **98** (2018) 85 [[1710.11155](#)].
- [69] Yu. A. Fomin, N. N. Kalmykov, I. S. Karpikov, G. V. Kulikov, M. Yu. Kuznetsov, G. I. Rubtsov et al., *No muon excess in extensive air showers at 100–500 PeV primary energy: EAS-MSU results*, *Astropart. Phys.* **92** (2017) 1 [[1609.05764](#)].
- [70] PIERRE AUGER collaboration, A. Aab et al., *Testing Hadronic Interactions at Ultrahigh Energies with Air Showers Measured by the Pierre Auger Observatory*, *Phys. Rev. Lett.* **117** (2016) 192001 [[1610.08509](#)].
- [71] G. R. Farrar and J. D. Allen, *A new physical phenomenon in ultra-high energy collisions*, *EPJ Web Conf.* **53** (2013) 07007 [[1307.2322](#)].
- [72] J. Alvarez-Muniz, L. Cazon, R. Conceicao, J. D. de Deus, C. Pajares and M. Pimenta, *Muon production and string percolation effects in cosmic rays at the highest energies*, [1209.6474](#).
- [73] PIERRE AUGER collaboration, A. Aab et al., *Inferences on mass composition and tests of hadronic interactions from 0.3 to 100 EeV using the water-Cherenkov*

- detectors of the Pierre Auger Observatory, *Phys. Rev. D* **96** (2017) 122003 [[1710.07249](#)].
- [74] PIERRE AUGER collaboration, A. Aab et al., *Observation of a Large-scale Anisotropy in the Arrival Directions of Cosmic Rays above 8×10^{18} eV*, *Science* **357** (2017) 1266 [[1709.07321](#)].
- [75] TELESCOPE ARRAY collaboration, H. Sagawa, *Telescope Array extension*, *Nucl. Part. Phys. Proc.* **279-281** (2016) 145.
- [76] T. Fujii et al., *Detection of ultra-high energy cosmic ray showers with a single-pixel fluorescence telescope*, *Astropart. Phys.* **74** (2016) 64 [[1504.00692](#)].
- [77] K. Fang et al., *The Giant Radio Array for Neutrino Detection (GRAND): Present and Perspectives*, *PoS ICRC2017* (2017) 996 [[1708.05128](#)].
- [78] A. V. Olinto et al., *POEMMA: Probe Of Extreme Multi-Messenger Astrophysics*, *PoS ICRC2017* (2017) 542 [[1708.07599](#)].
- [79] PIERRE AUGER collaboration, A. Aab et al., *The Pierre Auger Observatory Upgrade - Preliminary Design Report*, [1604.03637](#).
- [80] G. Parente and E. Zas, *Neutrino induced events in the Pierre Auger detector*, in *7th International Workshop on Neutrino Telescopes Venice, Italy, February 27-March 1, 1996*, 1996, [astro-ph/9606091](#).
- [81] K. S. Capelle, J. W. Cronin, G. Parente and E. Zas, *On the detection of ultrahigh-energy neutrinos with the Auger Observatory*, *Astropart. Phys.* **8** (1998) 321 [[astro-ph/9801313](#)].
- [82] F. Scheck, *Muon Physics*, *Phys. Rept.* **44** (1978) 187.
- [83] M. Davier, L. Duflo, F. Le Diberder and A. Rouge, *The Optimal method for the measurement of tau polarization*, *Phys. Lett. B* **306** (1993) 411.
- [84] ICECUBE collaboration, M. G. Aartsen et al., *Search for neutrino-induced particle showers with IceCube-40*, *Phys. Rev. D* **89** (2014) 102001 [[1312.0104](#)].
- [85] ICECUBE collaboration, M. G. Aartsen et al., *A combined maximum-likelihood analysis of the high-energy astrophysical neutrino flux measured with IceCube*, *Astrophys. J.* **809** (2015) 98 [[1507.03991](#)].
- [86] K. Greisen, *End to the cosmic ray spectrum?*, *Phys. Rev. Lett.* **16** (1966) 748.
- [87] G. T. Zatsepin and V. A. Kuzmin, *Upper limit of the spectrum of cosmic rays*, *JETP Lett.* **4** (1966) 78.
- [88] K. K. Andersen and S. R. Klein, *High energy cosmic-ray interactions with particles from the Sun*, *Phys. Rev. D* **83** (2011) 103519 [[1103.5090](#)].